

# Interstellar bromine abundance is consistent with cometary ices from Rosetta

N. F. W. Ligterink<sup>1,2</sup> and M. Kama<sup>3,1</sup>

<sup>1</sup> Leiden Observatory, Leiden University, PO Box 9513, 2300 RA Leiden, The Netherlands  
e-mail: ligterink@strw.leidenuniv.nl

<sup>2</sup> Raymond and Beverly Sackler Laboratory for Astrophysics, Leiden Observatory, Leiden University, PO Box 9513, 2300 RA Leiden, The Netherlands

<sup>3</sup> Institute of Astronomy, University of Cambridge, Madingley Road, Cambridge CB3 0HA, UK  
e-mail: mkama@ast.cam.ac.uk

Received 20 November 2017 / Accepted 23 February 2018

## ABSTRACT

**Context.** Cometary ices are formed during star and planet formation, and their molecular and elemental makeup can be related to the early solar system via the study of inter- and protostellar material.

**Aims.** We set out to place the first observational constraints on the interstellar gas-phase abundance of bromine (Br). We further aim to compare the protostellar Br abundance with that measured by Rosetta in the ices of comet 67P/Churyumov–Gerasimenko.

**Methods.** Archival *Herschel* data of Orion KL, Sgr B2(N), and NGC 6334I are examined for the presence of HBr and HBr<sup>+</sup> emission or absorption lines. A chemical network for modelling HBr in protostellar molecular gas is compiled to aid in the interpretation.

**Results.** HBr and HBr<sup>+</sup> were not detected towards any of our targets. However, in the Orion KL Hot Core, our upper limit on HBr/H<sub>2</sub>O is a factor of ten below the ratio measured in comet 67P. This result is consistent with the chemical network prediction that HBr is not a dominant gas-phase Br carrier. Cometary HBr is likely predominantly formed in icy grain mantles which lock up nearly all elemental Br.

**Key words.** astrochemistry – techniques: spectroscopic – molecular processes – stars: protostars – ISM: molecules

## 1. Introduction

Observations of halogen-bearing species in molecular gas can probe the gas-to-ice depletion of volatile elements during star and planet formation (Gerin et al. 2016). Previous studies have characterized the abundance of fluorine (F) and chlorine (Cl) in protostellar gas. We analyse archival data from the *Herschel* Space Observatory to constrain the gas-phase abundance budget of bromine (Br) and thus expand the overall knowledge of interstellar halogen chemistry. With the recent detection of the organohalogen CH<sub>3</sub>Cl (Fayolle et al. 2017), constraints on the abundances of Br could also give information on the presence of organobromine compounds in the interstellar medium.

The solar abundances of F and Cl are  $(3.63 \pm 0.11) \times 10^{-8}$  and  $(3.16 \pm 0.95) \times 10^{-7}$ , respectively (Asplund et al. 2009). The gas-phase HCl abundance in dense protostellar cores is  $[\text{HCl}/\text{H}_2] \sim 10^{-10}$ , with Cl depleted by a factor 100–1000 (Blake et al. 1985; Schilke et al. 1995; Zmuidzinas et al. 1995; Salez et al. 1996; Neufeld & Green 1994; Peng et al. 2010; Kama et al. 2015). Models indicate that the missing Cl is in HCl ice (Kama et al. 2015). A high Cl fraction in HCl ice was confirmed in situ for comet 67P/Churyumov–Gerasimenko (hereafter 67P/C–G) with Rosetta, which recently measured  $\text{HCl}/\text{H}_2\text{O} \approx 1.2 \times 10^{-4}$  (Dhooghe et al. 2017), close to *Herschel* upper limits at comets Hartley 2 and Garradd (Bockelée-Morvan et al. 2014).

In contrast to F and Cl, the solar and interstellar Br abundance is unknown, but in meteorites it is equivalent to

$\text{Br}/\text{H} = (3.47 \pm 0.02) \times 10^{-10}$  (Lodders et al. 2009). The two stable isotopes of bromine are <sup>79</sup>Br and <sup>81</sup>Br, with a terrestrial abundance ratio of <sup>79</sup>Br/<sup>81</sup>Br = 1.03 (Böhlke et al. 2005). For comet 67P/C–G, the Rosetta spacecraft detected HBr and measured an elemental ratio of  $\text{Br}/\text{O} = (1 - 7) \times 10^{-6}$  in the inner coma, consistent with nearly all bromine being locked in ice, analogously to chlorine.

Accounting for the range of variation seen in 67P/C–G and the uncertainties in terrestrial data, the cometary Br/Cl value of  $\approx 0.02$  (Dhooghe et al. 2017) is consistent with the bulk Earth estimate of  $\text{Br}/\text{Cl} \approx 0.04$  (Allègre et al. 2001).

If Br has a similar depletion level as Cl in protostellar gas, it may be detectable as HBr at a sensitivity of  $\delta T \lesssim 0.01 \times T(\text{HCl})$ , where  $T$  is the intensity in kelvin. The lowest rotational transitions of HBr are at around 500, 1000, and 1500 GHz. These frequencies are not observable from the ground, but were covered by the *Herschel*/HIFI spectrometer. We also consider the potentially abundant molecular ion HBr<sup>+</sup>. During regular science observations, HIFI serendipitously covered transitions of HBr and HBr<sup>+</sup> towards the bright protostellar regions Orion KL, Sagittarius B2 North (hereafter Sgr B2(N)), and NGC6334I. We use these data to constrain the gas-phase abundance of Br-carriers.

In Sect. 2, we summarise the spectroscopy and the archival *Herschel* data, which are analysed and discussed in Sect. 3. Section 4 compares the interstellar observations with cometary detections in 67P/C–G. In Sect. 5, we review the interstellar chemistry of Br. Our conclusions are presented in Sect. 6.

**Table 1.** Source parameters in HIFI band 1a.

| Source                      | $\theta_S$<br>'' | RMS<br>(mK) | $V_{\text{LSR}}$<br>(km s <sup>-1</sup> ) | $\Delta V$<br>(km s <sup>-1</sup> ) | $3\sigma$ Flux<br>(mK km s <sup>-1</sup> ) | Continuum<br>(K) | Mean $T_{\text{ex}}$<br>(K) |
|-----------------------------|------------------|-------------|---|-------------------------------------|--|------------------|-----------------------------|
| Orion KL <sup>a</sup> Plat. | 30               | 23.0        | 7–11                                      | ≥20                                 | 364  | 1.6              | 94                          |
| Orion KL HC                 | 10               | 23.0        | 4–6                                       | 7                                   | 216  | 1.6              | 155                         |
| Orion KL CR                 | 10               | 23.0        | 7–9                                       | 6                                   | 200  | 1.6              | 138                         |
| Sgr B2(N) <sup>b</sup> HC   | ~5               | 29.3        | 50–100                                    | 9                                   | 311  | 2.5              | 144                         |
| Sgr B2(N) env.              | –                | 29.3        | 50–100                                    | 20                                  | 464  | 2.5              | 34                          |
| NGC6334I <sup>c</sup> HC    | ~5               | 7.8         | –20–7                                     | 4                                   | 55   | 1.0              | 90                          |
| NGC6334I env.               | 20*              | 7.8         | –20–7                                     | 8                                   | 78   | 1.0              | 22                          |

**Notes.** Plat. – Plateau, HC – Hot Core, CR – Compact Ridge, env. – envelope. <sup>(a)</sup>Crockett et al. (2014a), <sup>(b)</sup>Neill et al. (2014), <sup>(c)</sup>Zernickel et al. (2012), <sup>(\*)</sup>based on the derived HCl source size. Mean excitation temperatures are derived from detected species in publications <sup>(a,b,c)</sup>.

## 2. Data

### 2.1. Spectroscopy of HBr and HBr<sup>+</sup>

Measurements on rotational lines of HBr were performed by Van Dijk & Dymanus (1969) for the hyperfine components of the first rotational transition and later extended by Di Lonardo et al. (1991) up to  $J_u = 9$ . The first three rotational transitions of both H<sup>79</sup>Br and H<sup>81</sup>Br are found at frequencies just above 500, 1000, and 1500 GHz, respectively (Table A.1). The three lowest rotational transitions of HBr<sup>+</sup> are found at 1188.2, 1662.7, and 2136.8 GHz and also display hyperfine splitting (Saykally & Evenson 1979; Lubic et al. 1989). However, insufficient spectroscopic data of HBr<sup>+</sup> are available to determine column densities. The lowest HBr and HBr<sup>+</sup> transition frequencies fall in spectral regions with heavy atmospheric absorption and are best observed from space.

### 2.2. Archival Herschel observations and selected sources

The *Herschel* Space Observatory mission (Pilbratt et al. 2010), active from 2009 to 2013, was the most sensitive observatory to date in the terahertz frequency range. We investigate archival high spectral resolution and broad wavelength coverage data from its heterodyne instrument, HIFI (de Graauw et al. 2010).

The HEXOS guaranteed-time key program (PI E.A. Bergin, Bergin et al. 2010) obtained full spectral scans of Orion KL and Sgr B2 (Crockett et al. 2014a,b; Neill et al. 2014), covering three rotational transitions of HBr in HIFI bands 1a, 4a and 6a and HBr<sup>+</sup> transitions in band 5a and 6b. The CHESS key program (PI C. Ceccarelli, Ceccarelli et al. 2010) observed NGC6334I in the same HIFI bands (Zernickel et al. 2012). These three sources are bright and well-studied, and have yielded strong detections of the halogens HF and HCl with the latter having integrated intensities of  $\int T_{mb} dv = 701.9$  K km s<sup>-1</sup> over two lines for Orion KL and  $\int T_{mb} dv = 40$  K km s<sup>-1</sup> over three lines for NGC6334I. Line intensities one to two orders of magnitude lower than the HCl peak brightness should be detectable, based on  $3\sigma$  noise levels of  $\sim 0.36$  K km s<sup>-1</sup> and  $\sim 0.08$  K km s<sup>-1</sup> for these sources, respectively. The observational details of these three sources are listed in Table 1.

### 2.3. Analysis method

All sources are inspected for features corresponding to transitions of H<sup>79/81</sup>Br and HBr<sup>+</sup> using the Weeds addition (Maret et al. 2011) of the Continuum and Line Analysis Single-dish

Software (CLASS<sup>1</sup>). For line identification, we use the JPL<sup>2</sup> (Pickett et al. 1998) and CDMS<sup>3</sup> (Müller et al. 2001, 2005) spectroscopy databases. Source velocities matching previous detections of halogen-bearing molecules are considered most relevant, but we explore a large  $V_{\text{LSR}}$  range to check for emission or absorption components matching the hyperfine pattern. For emission features, the total column density  $N_T$  of a species can be calculated by assuming local thermodynamic equilibrium (LTE):

$$\frac{3k_B \int T_{\text{MB}} dV}{8\pi^3 \nu \mu^2 S} = \frac{N_{\text{up}}}{g_{\text{up}}} = \frac{N_T}{Q(T_{\text{rot}})} e^{-E_{\text{up}}/T_{\text{rot}}}, \quad (1)$$

where  $\int T_{\text{MB}} dV$  is the integrated main-beam intensity of a spectral line,  $\nu$  the transition frequency,  $\mu^2$  the dipole moment,  $S$  the transition strength,  $g_{\text{up}}$  the upper state degeneracy,  $Q(T_{\text{rot}})$  the rotational partition function,  $E_{\text{up}}$  the upper state energy and  $T_{\text{rot}}$  the rotational temperature. Upper limits are given at  $3\sigma$  confidence and calculated by  $\sigma = 1.1 \sqrt{\delta\nu \Delta V} \times \text{RMS}$ , where  $\delta\nu$  is the velocity resolution,  $\Delta V$  the line width (estimated based on other transitions in the spectrum) and RMS the root mean square noise in Kelvin. A factor of 1.1 accounts for the flux calibration uncertainty of 10% (Roelfsema et al. 2012).

In the source sample, the hydrogen halides HF and HCl are also found in absorption. We calculate the column density corresponding to absorption features from:

$$\tau = -\ln\left(\frac{T_{\text{MB}}}{T_{\text{cont}}}\right), \quad (2)$$

and

$$N_T = \frac{8\pi^{3/2} \times \Delta V}{2 \sqrt{\ln 2} \times \lambda^3} \frac{g_l}{g_u} \times \tau, \quad (3)$$

where  $\tau$  is the optical depth,  $T_{\text{MB}}$  the brightness temperature of the feature and  $T_{\text{cont}}$  the continuum level.  $\lambda$  is the wavelength of the transitions and  $g_l$  and  $g_u$  are its lower and upper state degeneracies. For non-detections, a  $3\sigma$  upper limit column density is determined using  $T_{\text{MB}} = T_{\text{cont}} - 3 \times \text{RMS}$  and assuming  $\Delta V$  equals the average line width for other species in the source.

<sup>1</sup> <http://www.iram.fr/IRAMFR/GILDAS>

<sup>2</sup> <http://spec.jpl.nasa.gov>

<sup>3</sup> <http://www.astro.uni-koeln.de/cdms>

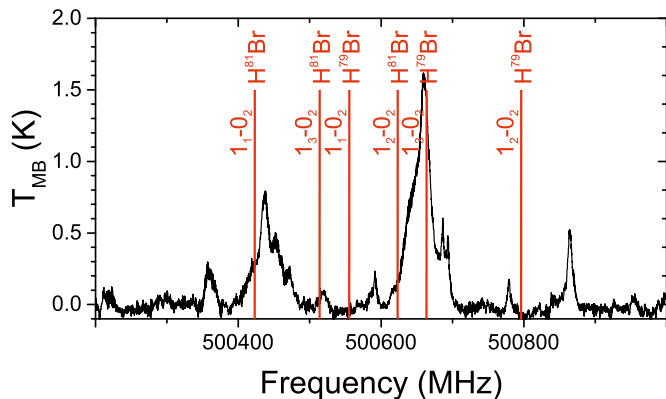


**Fig. 1.** Positions of the  $J = 1_x \rightarrow 0_2$  transitions of  $\text{H}^{79}\text{Br}$  and  $\text{H}^{81}\text{Br}$  at 500 GHz towards Orion KL for  $V_{\text{LSR}} = 9 \text{ km s}^{-1}$ .

If the source does not fill the entire HIFI beam (at 500 GHz,  $\theta_B = 44''$ ), we correct the column densities for beam dilution by applying the factor  $\eta_{\text{BF}} = \theta_S^2 / (\theta_S^2 + \theta_B^2)$ , where  $\theta_S$  is the source size and  $\theta_B$  the beam size. Source sizes are taken from literature, see Table 1, and are used as the physical size of the emitting regions. Deviations from the actual emitting area of a species may occur and would result in different column densities. The source-averaged column density is calculated from  $N_S = N_T / \eta_{\text{BF}}$ .

We determined the upper limit column densities from the HBr  $J = 1_x \rightarrow 0_2$  transitions at 500 GHz in HIFI band 1a, because of the low noise levels in this frequency range. HBr is considered as the sum of its isotopologs,  $\text{H}^{79}\text{Br}$  and  $\text{H}^{81}\text{Br}$ . We assume that the cosmic and local isotope ratios are equal (in the solar system  $[\text{H}^{79}\text{Br}] / [\text{H}^{81}\text{Br}] = 1.03$ ). Aside from the molecular mass, several spectroscopic parameters for transitions of both isotopes, such as  $A_{ij}$  and  $E_{\text{up}}$ , are identical. The  $1_3 \rightarrow 0_2$  line is the strongest hyperfine component and constrains the column density the most and is therefore used to give the most stringent upper limits.

### 3. Search for HBr and HBr<sup>+</sup> in the *Herschel* spectra

Analysis of the HIFI spectra of Orion KL, Sgr B2(N), and NGC6334I yielded no detections of HBr or HBr<sup>+</sup> features in emission or absorption. Figure 1 shows the positions of the HBr transitions at 500 GHz in the Orion KL spectrum at  $V_{\text{LSR}} = 9 \text{ km s}^{-1}$ , corresponding to the average velocity of the Plateau components. The data were analysed over a large range of source velocities, mainly focussing on velocities of known components. For Sgr B2(N) and NGC6334I the same figures can be found in Appendix B.

### 4. Protostellar versus cometary abundance

The upper limit abundance ratios of HBr toward the protostellar sources can be compared with measurements taken by the Rosetta mission of the coma gas of comet 67P/C-G (Dhooghe et al. 2017). We look at column density ratios of HBr (Table C.1) with respect to those of  $\text{H}_2$ ,  $\text{H}_2\text{O}$ ,  $\text{CH}_3\text{OH}$ , HF, and HCl (Table C.2). The  $N(\text{H}^{79+81}\text{Br}) / N(\text{X})$  column density ratios based either on emission or absorption upper limits for Orion KL, Sgr B2(N), and NGC6334I are listed in Table 2.

The upper limits in emission are based on an excitation temperature of 100 K, which is chosen to be within a factor of a few of all the detected molecules we compare with. For an assessment of the impact of  $T_{\text{ex}}$ , Fig. C.1 shows the temperature

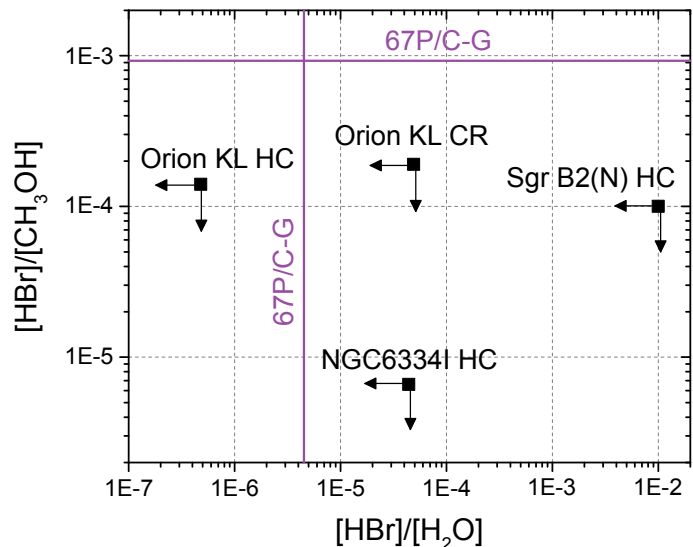


**Fig. 2.** (H)Br/ $\text{CH}_3\text{OH}$  and (H)Br/ $\text{H}_2\text{O}$  ratios plotted for 67P/C-G (purple lines, Dhooghe et al. 2017) and the upper limits on these ratios for the protostar sample (this work).

dependence of the  $3\sigma$  upper limit for the first three hyperfine transitions of  $\text{H}^{79/81}\text{Br}$ , including beam dilution correction for the Orion KL Hot Core. For Sgr B2(N) and NGC6334I, a distinction is made between the hot core and envelope components. If a source contains multiple kinematic components of a species, we adopt the dominant one.

For 67P/C-G, Dhooghe et al. (2017) give the Br/O ratio and the  $\text{CH}_3\text{OH}$  abundance. The cometary halogens are equal to the halides (HX), but the O abundance is the sum of  $\text{H}_2\text{O}$ , CO,  $\text{CO}_2$  and  $\text{O}_2$ . For the comet, we can therefore take  $\text{Br} \equiv \text{HBr}$ , and we further assume  $\text{O} \approx \text{H}_2\text{O}$ . A ratio of  $\text{CH}_3\text{OH}/\text{H}_2\text{O} = 3.1 - 5.5 \times 10^{-3}$  has been measured by Le Roy et al. (2015).

A comparison of HBr with  $\text{H}_2\text{O}$  and  $\text{CH}_3\text{OH}$  is shown in Fig. 2, and the full set of abundance ratios of HBr with other molecules is given in Table 2. The HBr/ $\text{CH}_3\text{OH}$  ratio in all our targets is constrained to be below that in comet 67P/C-G. This is not necessarily due to a particularly high methanol abundance in our targets, but rather could signify a low fraction of Br atoms locked up in gas-phase HBr molecules. The only source where we can constrain the HBr/ $\text{H}_2\text{O}$  ratio to be below that in 67P/C-G is the Orion KL Hot Core. This may, again, be explained with a low fraction of Br atoms in gas-phase HBr. If all elemental bromine were in gaseous HBr, we would have expected to have made a detection in the Orion KL Hot Core. A comparison with the cometary measurements suggests, then, that the HBr molecules are formed in icy grain mantles, rather than in the gas phase, or sublimate from the grain surface at a temperature higher than water.

The HBr/HCl abundance ratio in the Orion KL Plateau is constrained to be a factor  $\geq 4$  below that in 67P/C-G. The difficulties in forming a large abundance of HBr in the gas phase when HCl is clearly present lead us to conclude that cometary HBr has an origin in grain surface chemistry in volatile-rich ice mantles.

### 5. Interstellar chemistry of Br

#### 5.1. Reactions of Br

The inter- and protostellar chemistry of bromine is poorly characterized, compared to that of fluorine and chlorine

**Table 2.** Abundance ratios of  $H^{79+81}Br$  ( $\equiv B$ ) upper limit column density with  $H_2$ ,  $CH_3OH$ ,  $H_2O$ ,  $HF$ , and  $H^{35+37}Cl$  ( $\equiv HCl$ ) for Orion KL, Sgr B2(N), and NGC6334I, compared with abundance ratios derived for 67P/C-G.

| Source                      | B/ $H_2$                   | B/ $H_2O$                                       | B/ $CH_3OH$                        | B/ $HF$                            | B/ $HCl$                            |
|-----------------------------|----------------------------|---|------------------------------------|------------------------------------|-------------------------------------|
| Orion KL <sup>a</sup> Plat. | $\leq 8.9 \times 10^{-11}$ | $\leq 1.9 \times 10^{-5}$                       | –                                  | $\leq 1.2 \times 10^1$ *           | $\leq 1.3 \times 10^{-2}$           |
| Orion KL HC                 | $\leq 3.1 \times 10^{-10}$ | $\leq 4.8 \times 10^{-7}$                       | $\leq 1.4 \times 10^{-4}$          | –                                  | –                                   |
| Orion KL CR                 | $\leq 2.3 \times 10^{-10}$ | $\leq 4.9 \times 10^{-5}$                       | $\leq 1.9 \times 10^{-4}$          | –                                  | –                                   |
| Sgr B2(N) <sup>b</sup> HC   | $\leq 6.5 \times 10^{-11}$ | $\leq 1.0 \times 10^{-2}$                       | $\leq 1.0 \times 10^{-4}$          | –                                  | –                                   |
| Sgr B2(N) env.              | –                          | –   | $\leq 1 \times 10^{-3}$            | $\leq 1.1 \times 10^{-1}$ *        | $\leq 6.9 \times 10^{-2}$ *         |
| NGC6334I <sup>c</sup> HC    | $\leq 8.4 \times 10^{-11}$ | $\leq 4.4 \times 10^{-5}$                       | $\leq 6.6 \times 10^{-6}$          | –                                  | $\leq 4.8 \times 10^{-1}$           |
| NGC6334I env.               | –                          | –   | –                                  | $\leq 2.0 \times 10^{-1}$ *        | $\leq 9.3 \times 10^{-1}$ *         |
| 67P/C-G <sup>d</sup>        | –                          | $4.5^{+3.5}_{-3.5} \times 10^{-6}$ <sup>e</sup> | $1.4^{+1.2}_{-0.7} \times 10^{-3}$ | $1.7^{+5.1}_{-1.3} \times 10^{-2}$ | $4.8^{+13.8}_{-3.7} \times 10^{-2}$ |

**Notes.** Plat. – Plateau, HC – Hot Core, CR – Compact Ridge, env. – envelope. <sup>(a)</sup>Crockett et al. (2014a); <sup>(b)</sup>Neill et al. (2014); <sup>(c)</sup>Zernickel et al. (2012); <sup>(d)</sup>Dhooghe et al. (2017); <sup>(e)</sup>Br/O elemental ratio, O has contributions of water, but also CO, CO<sub>2</sub> and O<sub>2</sub>; \* indicates values based on an upper limit in absorption, other values are based on the emission upper limits.

**Table 3.** Chemical reaction network for bromine.

| #    | $R_1$     | $R_2$  | $P_1$     | $P_2$ | $k(T)$ [ $cm^3 s^{-1}$ ]                             | Reference  |
|------|-----------|--------|-----------|-------|--|--|
| (1)  | Br        | $H_2$  | HBr       | H     | $8.3 \times 10^{-11} \times \exp(-8812 \text{ K}/T)$ | Fettis et al. (1960)   |
| (2)  | HBr       | H      | Br        | $H_2$ | $8.9 \times 10^{-11} \times \exp(-684 \text{ K}/T)$  | White & Thompson (1974)  |
| (3)  | HBr       | $H'$   | $H'Br$    | H     | $4.0 \times 10^{-10} \times \exp(-1140 \text{ K}/T)$ | White & Thompson (1974)  |
| (4)  | $Br^+$    | $H_2$  | $HBr^+$   | H     | $10^{-9} \times \exp(-6200 \text{ K}/T)$             | Mayhew & Smith (1990), Neufeld & Wolfire (2009) <sup>a,c</sup> |
| (5)  | $HBr^+$   | $e^-$  | Br        | H     | $2 \times 10^{-7} \times (T/300 \text{ K})^{-0.5}$   | Neufeld & Wolfire (2009) <sup>a</sup>                          |
| (6)  | $HBr^+$   | $H_2$  | $H_2Br^+$ | H     | $(13.2 \pm 1.6) \times 10^{-10}$                     | Belikov & Smith (2008)   |
| (7)  | $H_2Br^+$ | $e^-$  | HBr       | H     | $\leq 10^{-8} \times (T/300 \text{ K})^{-0.85}$      | Neufeld & Wolfire (2009) <sup>a,b</sup>                        |
| (8)  | $H_2Br^+$ | $e^-$  | Br        | 2H    | $\sim 10^{-7} \times (T/300 \text{ K})^{-0.85}$      | Neufeld & Wolfire (2009) <sup>a</sup>                          |
| (9)  | HBr       | $h\nu$ | Br        | H     | $1.7 \times 10^{-7} \times \chi_{UV}$                | Neufeld & Wolfire (2009) <sup>a</sup>                          |
| (10) | HBr       | $h\nu$ | $HBr^+$   | $e^-$ | $10^{-10} \times \chi_{UV}$                          | Neufeld & Wolfire (2009) <sup>a</sup>                          |

**Notes.**  $R_i$  and  $P_i$  denote the reactants and products. <sup>(a)</sup>Assumed order-of-magnitude similar to corresponding  $Cl$ , F reactions from Neufeld & Wolfire (2009); <sup>(b)</sup>upper limit based on  $H_2Cl^+ + e^-$  branching ratio (see text); <sup>(c)</sup>see Sect. 5.

(e.g. Jura 1974; Blake et al. 1986; Schilke et al. 1995; Neufeld & Wolfire 2009). In Table 3, we present a network compiled from published measurements and calculations, with missing data filled in with values from the  $Cl$  and F networks. Some reactions are not listed in this table, for these reactions we adopt the equivalent  $Cl$  reaction parameters of Neufeld & Wolfire (2009, their Table 1).

The neutral-neutral chemistry, reactions (1) to (3), is relatively well studied. The  $Br+H_2$  reaction leading to  $HBr+H$ , with an 8812 K activation energy, has been investigated by, for example, Eyring (1931); Plooster & Garvin (1956) and Fettis et al. (1960). The  $HBr+H$  abstraction and exchange reactions have been studied by Plooster & Garvin (1956), and by White & Thompson (1974) whose channel-by-channel rates are consistent with the total rate from Endo & Glass (1976). Based on Table 3, excluding other reactions, the competition between the  $Br+H_2$  formation route and destruction via the  $HBr+H$  abstraction reaction strongly favours atomic Br. Thus gas-phase neutral-neutral chemistry is not expected to contribute to HBr formation unless temperatures of  $\sim 1000$  K – possible in hot cores, outflow shocks, and inner regions of protoplanetary disks – are involved.

Due to its low first ionization potential (11.8 eV), Br is easily ionized and HBr can form in ion-neutral chemistry via the set of reactions (4)–(8) in Table 3. By analogy with F and  $Cl$ , reactions (4)–(8) should be fast, of order

$10^{-10}$ – $10^{-7} \text{ cm}^3 \text{ s}^{-1}$  (Neufeld & Wolfire 2009). However, as pointed out by Mayhew & Smith (1990), the  $Br^++H_2$  reaction is endothermic. We adopt a  $H_2$  and  $HBr^+$  dissociation energy ( $E_D$ ) difference of  $\approx 6200$  K, estimated from the proton affinity (PA) and ionization potential (IP) of Br via  $E_a = PA(Br) + IP(Br) - IP(H_2) - E_D(H_2)$ , suggested by D. Neufeld (priv. comm.). The branching ratio of the dissociative recombination reactions (7) and (8) is unknown, but the dissociation energy of HBr ( $D_0 \approx 3.78$  eV) is lower than that of  $H_2$  (4.48 eV), while those of  $HCl$  and  $HF$  are similar and higher (4.43 and 5.87 eV, Darwent 1970). The branching ratio into the  $HBr+H$  channel may thus be lower than the 10 % of the equivalent  $Cl$  reaction, which would lower the fraction of Br stored in HBr. For the photoionization and -dissociation rates, we adopt order-of-magnitude numbers from the corresponding  $Cl$  and F reactions in Neufeld & Wolfire (2009).

The formation of HBr via  $H+Br$  collision requires a three-body interaction and thus is most efficient on grain surfaces (e.g. Ree et al. 2004).

## 5.2. Chemical modelling results

We appended the reactions from Table 3 to the OSU2009 network and ran time-dependent, gas-phase only simulations to 1.5 Myr with the Astrochem gas-phase chemistry code (Maret & Bergin 2015). We ignored freeze-out in order to test

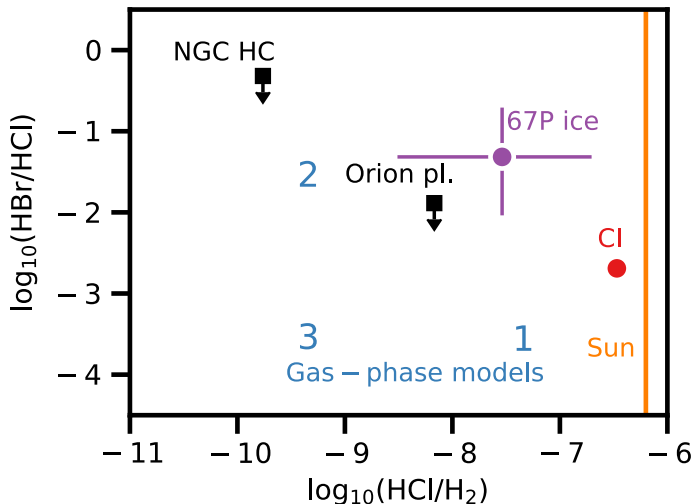


**Fig. 3.** Ratio of HBr to HCl abundance in the NGC 6334I Hot Core and the Orion KL Plateau (upper limits for both sources) and pure gas-phase chemical models (1, 2, 3; see text), and in comet 67P/C–G (Dhooghe et al. 2017). We also show the elemental Cl/H<sub>2</sub> and Br/Cl ratios for meteorites (red circle) and the sun (orange line; the solar Br abundance is unknown). Models are shown for  $n_{\text{H}} = 10^6 \text{ cm}^{-3}$  and  $T_{\text{kin}} = 150 \text{ K}$ . Variations of  $\pm 1$  in  $\log(n_{\text{H}})$  and  $\pm 50 \text{ K}$  in  $T_{\text{kin}}$  induce negligible and 0.5 dex variations, respectively. Model 1 has all elemental Cl and Br in the gas; in 2 only Cl, and in 3 both Cl and Br are depleted from the gas by a factor of 100.

the relevance of the *Herschel* upper limits with the highest possible gas-phase elemental abundances. The physical conditions were set to  $A_{\text{V}} = 20 \text{ mag}$  (assuming a standard interstellar radiation field),  $n_{\text{H}} = 10^6 \text{ cm}^{-3}$ , and  $T_{\text{kin}} = 150 \text{ K}$ . The initial halogen abundances were either entirely atomic ions ( $\text{Cl}^+$  and  $\text{Br}^+$ ) or entirely diatomic hydrides (HCl and HBr), but this had only a minor impact on the end-state abundances. We show the modelling results in Fig. 3 for three cases: 1) all elemental Br and Cl in the gas-phase; 2) undepleted Br and Cl depleted from the gas-phase by two orders of magnitude 3) both Br and Cl depleted by two orders of magnitude. Varying  $n_{\text{H}}$  by an order of magnitude had little impact on the abundances, while varying  $T_{\text{kin}}$  by 50 K induced a scatter of 0.5 dex in the plotted logarithmic abundance ratios. None of the models were strongly constrained by the upper limits, as we discuss below.

For the adopted physical conditions, the chemical network predictions place the gas-phase HBr abundance two orders of magnitude below the observed upper limit for the Orion KL Hot Core. All literature studies of the gas-phase Cl abundance in protostellar sources find gas-phase Cl depletions of at least a factor 100 to 1000 (Dalgarno et al. 1974; Blake et al. 1986; Schilke et al. 1995; Peng et al. 2010; Kama et al. 2015). However, the ice fraction in the Orion KL Hot Core is likely very small, so we expect model 1 to provide a reasonable prediction of the gas-phase (H)Cl and (H)Br abundance in this source.

In the NGC 6334I Hot Core, HBr may be just below the upper limit from *Herschel* if elemental Br is not depleted from the gas, while Cl is known to be depleted by a factor 1000. This seems unlikely.

## 6. Conclusions

We present the first search for bromine-bearing molecules in the interstellar medium, employing archival *Herschel*/HIFI data. No detections of HBr or  $\text{HBr}^+$  are made, and we report upper limits

of HBr for Orion KL, Sgr B2 (N), and NGC 6334I. Most of these upper limits lie above the values expected from a simple scaling down of HCl emission using the Cl/Br elemental ratio.

In the Orion KL Hot Core, the HBr/H<sub>2</sub>O gas-phase abundance ratio is constrained to be an order of magnitude lower than the measured ratio in comet 67P/C–G. This result, along with the low HBr/CH<sub>3</sub>OH ratio in all our sources and the low HBr/HCl in the Orion KL Plateau, is consistent with our chemical network modelling for Br, which predicts a low fraction of elemental Br in HBr in the gas phase. Our results suggest the HBr detected in high abundance in comet 67P/C–G formed in icy grain mantles.

*Acknowledgements.* The authors wish to thank Nathan Crockett for providing the data on Orion KL and Sgr B2, and Peter Schilke for the data on NGC6334I. We also thank Frederik Dhooghe for discussing his results on halogens in 67P/C–G and David Neufeld and Catherine Walsh for discussions on the chemistry. MK is supported by an Intra-European Marie Skłodowska-Curie Fellowship. Astrochemistry in Leiden is supported by the Netherlands Research School for Astronomy (NOVA), by a Royal Netherlands Academy of Arts and Sciences (KNAW) professor prize, and by the European Union A-ERC grant 291141 CHEMPLAN. HIFI has been designed and built by a consortium of institutes and university departments from across Europe, Canada and the United States under the leadership of SRON Netherlands Institute for Space Research, Groningen, The Netherlands and with major contributions from Germany, France and the US. Consortium members are: Canada: CSA, UWaterloo; France: CESR, LAB, LERMA, IRAM; Germany: KOSMA, MPIFR, MPS; Ireland: NUI Maynooth; Italy: ASI, IFSI-INAF, Osservatorio Astrofisico di Arcetri-INAF; Netherlands: SRON, TUD; Poland: CAMK, CBK; Spain: Observatorio Astronómico Nacional (IGN), Centro de Astrobiología (CSIC-INTA). Sweden: Chalmers University of Technology - MC2, RSS & GARD; Onsala Space Observatory; Swedish National Space Board, Stockholm University - Stockholm Observatory; Switzerland: ETH Zurich, FHNW; USA: Caltech, JPL, NHSC.

## References

- Allègre, C., Manhès, G., & Lewin, É. 2001, *Earth Planet. Sci. Lett.*, **185**, 49
- Asplund, M., Grevesse, N., Sauval, A. J., & Scott, P. 2009, *ARA&A*, **47**, 481
- Belikov, A. E., & Smith, M. A. 2008, *Russ. J. Phys. Chem. A*, **82**, 789
- Bergin, E. A., Phillips, T. G., Comito, C., et al. 2010, *A&A*, **521**, L20
- Blake, G. A., Keene, J., & Phillips, T. G. 1985, *ApJ*, **295**, 501
- Blake, G. A., Anicich, V. G., & Huntress, Jr. W. T. 1986, *ApJ*, **300**, 415
- Bockelée-Morvan, D., Biver, N., Crovisier, J., et al. 2014, *A&A*, **562**, A5
- Böhlke, J. K., de Laeter, J. R., De Bièvre, P., et al. 2005, *J. Phys. Chem. Ref. Data*, **34**, 57
- Ceccarelli, C., Bacmann, A., Boogert, A., et al. 2010, *A&A*, **521**, L22
- Crockett, N. R., Bergin, E. A., Neill, J. L., et al. 2014a, *ApJ*, **781**, 114
- Crockett, N. R., Bergin, E. A., Neill, J. L., et al. 2014b, *ApJ*, **787**, 112
- Dalgarno, A., de Jong, T., Oppenheimer, M., & Black, J. H. 1974, *ApJ*, **192**, L37
- Darwent, B. d. 1970, *NIST Spec. Publ.*, **1**
- de Graauw, T., Helmich, F. P., Phillips, T. G., et al. 2010, *A&A*, **518**, L6
- Dhooghe, F., De Keyser, J., Altwegg, K., et al. 2017, *MNRAS*, **472**, 1336
- Di Lonardo, G., Fusina, L., De Natale, P., Inguscio, M., & Prevedelli, M. 1991, *J. Mol. Spectrosc.*, **148**, 86
- Endo, H., & Glass, G. 1976, *J. Phys. Chem.*, **80**, 1519
- Eyring, H. 1931, *J. Am. Chem. Soc.*, **53**, 2537
- Fayolle, E. C., Öberg, K. I., Jørgensen, J. K., et al. 2017, *Nat. Astron.*, **1**, 703
- Fettis, G., Knox, J., & Trotman-Dickenson, A. 1960, *Can. J. Chem.*, **38**, 1643
- Gerin, M., Neufeld, D. A., & Goicoechea, J. R. 2016, *ARA&A*, **54**, 181
- Jura, M. 1974, *ApJ*, **190**, L33
- Kama, M., Caux, E., López-Sepulcre, A., et al. 2015, *A&A*, **574**, A107
- Le Roy, L., Altwegg, K., Balsiger, H., et al. 2015, *A&A*, **583**, A1
- Lodders, K., Palme, H., & Gail, H.-P. 2009, *Landolt Börnstein Group VI Astronomy and Astrophysics Numerical Data and Functional Relationships in Science and Technology Volume 4B*
- Lubic, K. G., Ray, D., Hovde, D. C., Veseth, L., & Saykally, R. J. 1989, *J. Mol. Spectrosc.*, **134**, 21
- Maret, S., & Bergin, E. A. 2015, *Astrochem: Abundances of Chemical Species in the Interstellar Medium*, Astrophysics Source Code Library
- Maret, S., Hily-Blant, P., Pety, J., Bardeau, S., & Reynier, E. 2011, *A&A*, **526**, A47
- Mayhew, C. A., & Smith, D. 1990, *Int. J. Mass Spectrom. Ion Process.*, **100**, 737
- Müller, H. S. P., Thorwirth, S., Roth, D. A., & Winnewisser, G. 2001, *A&A*, **370**, L49
- Müller, H. S. P., Schlöder, F., Stutzki, J., & Winnewisser, G. 2005, *J. Mol. Struct.*, **742**, 215

- Neill, J. L., Bergin, E. A., Lis, D. C., et al. 2014, *ApJ*, 789, 8
- Neufeld, D. A., & Green, S. 1994, *ApJ*, 432, 158
- Neufeld, D. A., & Wolfire, M. G. 2009, *ApJ*, 706, 1594
- Peng, R., Yoshida, H., Chamberlin, R. A., et al. 2010, *ApJ*, 723, 218
- Pickett, H. M., Poynter, R. L., Cohen, E. A., et al. 1998, *J. Quant. Spec. Radiat. Transf.*, 60, 883
- Pilbratt, G. L., Riedinger, J. R., Passvogel, T., et al. 2010, *A&A*, 518, L1
- Plooster, M. N., & Garvin, D. 1956, *J. Am. Chem. Soc.*, 78, 6003
- Ree, J., Yoon, S., Park, K., & Kim, Y. 2004, *Bull. Korean Chem. Soc.*, 25, 1217
- Roelfsema, P. R., Helmich, F. P., Teyssier, D., et al. 2012, *A&A*, 537, A17
- Salez, M., Frerking, M. A., & Langer, W. D. 1996, *ApJ*, 467, 708
- Saykally, R. J., & Evenson, K. M. 1979, *Phys. Rev. Lett.*, 43, 515
- Schilke, P., Phillips, T. G., & Wang, N. 1995, *ApJ*, 441, 334
- Van Dijk, F. A., & Dymanus, A. 1969, *Chem. Phys. Lett.*, 4, 170
- White, J. M., & Thompson, D. L. 1974, *J. Chem. Phys.*, 61, 719
- Zernickel, A., Schilke, P., Schmiedeke, A., et al. 2012, *A&A*, 546, A87
- Zmuidzinas, J., Blake, G. A., Carlstrom, J., Keene, J., & Miller, D. 1995, *ApJ*, 447, L125

## Appendix A: Linelist of HBr transitions in range of HIFI

The HIFI instrument on the *Herschel* Space Observatory covered the three lowest rotational transition groups of HBr, which are summarised in Table A.1.  $J = 1_x \rightarrow 0_2$  fell in band 1a,  $J = 2_x \rightarrow 1_y$  in band 4a and  $J = 3_x \rightarrow 2_y$  in band 6a.

**Table A.1.**  $H^{79/81}Br$  transitions between 500 and 1501 GHz.

| $\nu$ $H^{79}Br$<br>(MHz) | $\nu$ $H^{81}Br$<br>(MHz) | A<br>( $s^{-1}$ ) | $E_{upper}$<br>(K) | $J', F'$       | $J'', F''$     |
|---------------------------|---------------------------|-------------------|--------------------|----------------|----------------|
| 500540.1280               | 500407.2010               | 3.34E-4           | 24.0               | 1 <sub>1</sub> | 0 <sub>2</sub> |
| 500647.7450               | 500497.3850               | 3.34E-4           | 24.0               | 1 <sub>3</sub> | 0 <sub>2</sub> |
| 500780.0980               | 500607.7750               | 3.34E-4           | 24.0               | 1 <sub>2</sub> | 0 <sub>2</sub> |
| 1000859.5610              | 1000589.5640              | 5.33E-4           | 72.1               | 2 <sub>1</sub> | 1 <sub>2</sub> |
| 1000993.2470              | 1000701.3110              | 1.71E-3           | 72.1               | 2 <sub>2</sub> | 1 <sub>2</sub> |
| 1001089.1700              | 1000781.6850              | 2.24E-3           | 72.1               | 2 <sub>3</sub> | 1 <sub>2</sub> |
| 1001089.1700              | 1000781.6850              | 3.20E-3           | 72.1               | 2 <sub>4</sub> | 1 <sub>3</sub> |
| 1001099.6240              | 1000790.3740              | 2.67E-3           | 72.1               | 2 <sub>1</sub> | 1 <sub>1</sub> |
| 1001125.5610              | 1000811.7800              | 1.60E-4           | 72.1               | 2 <sub>2</sub> | 1 <sub>3</sub> |
| 1001221.3420              | 1000891.7620              | 9.61E-4           | 72.1               | 2 <sub>3</sub> | 1 <sub>3</sub> |
| 1001233.1690              | 1000901.9040              | 1.33E-3           | 72.1               | 2 <sub>2</sub> | 1 <sub>1</sub> |
| 1500828.0700              | 1500397.4070              | 2.31E-4           | 144.1              | 3 <sub>2</sub> | 2 <sub>3</sub> |
| 1500923.7510              | 1500477.5790              | 3.24E-3           | 144.1              | 3 <sub>2</sub> | 2 <sub>2</sub> |
| 1500961.8100              | 1500509.4550              | 2.82E-3           | 144.1              | 3 <sub>3</sub> | 2 <sub>3</sub> |
| 1501025.2220              | 1500562.4860              | 9.91E-3           | 144.1              | 3 <sub>4</sub> | 2 <sub>3</sub> |
| 1501025.2220              | 1500562.4860              | 1.16E-2           | 144.1              | 3 <sub>5</sub> | 2 <sub>4</sub> |
| 1501057.6120              | 1500589.4380              | 8.10E-3           | 144.1              | 3 <sub>2</sub> | 2 <sub>1</sub> |
| 1501057.6120              | 1500589.4380              | 8.64E-3           | 144.1              | 3 <sub>3</sub> | 2 <sub>2</sub> |
| 1501094.0810              | 1500619.5480              | 1.10E-4           | 144.1              | 3 <sub>3</sub> | 2 <sub>4</sub> |
| 1501157.1420              | 1500672.5180              | 1.65E-3           | 144.1              | 3 <sub>4</sub> | 2 <sub>4</sub> |

## Appendix B: Sgr B2(N) and NGC6334I at 500 GHz

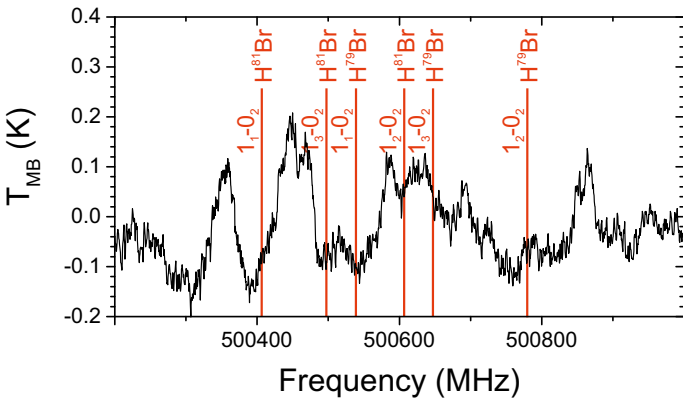


**Fig. B.1.** Positions of  $H^{79/81}Br$  transitions for  $J = 1_x \rightarrow 0_2$  around 500 GHz in HIFI band 1a towards Sgr B2(N) for  $V_{LSR} = 64 \text{ km s}^{-1}$ .

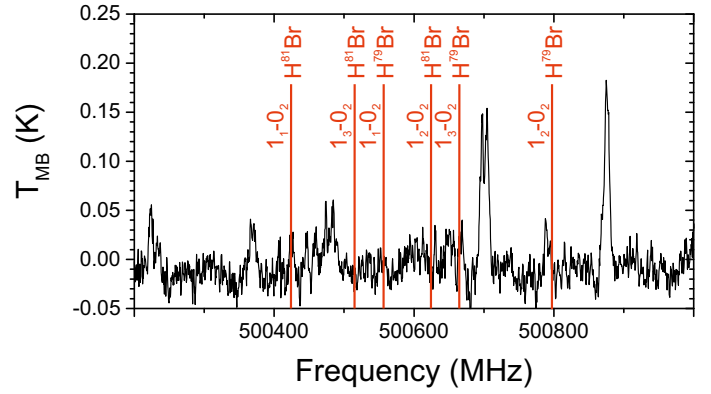


**Fig. B.2.** Positions of  $H^{79/81}Br$  transitions for  $J = 1_x \rightarrow 0_2$  around 500 GHz in HIFI band 1a towards NGC6334I for  $V_{LSR} = -10 \text{ km s}^{-1}$ .

## Appendix C: Upper limit column densities of $H^{79+81}Br$ and column densities of reference molecules

Table C.1 lists the upper limit column densities of  $H^{79+81}Br$  for the full HIFI band 1a beam ( $=44''$ ) in emission and absorption, calculated according to Eqs. (1) and (3). Upper limits have been derived for an excitation temperature of 100 K. The following columns in this table list the beam dilution correction factor and subsequently the beam dilution corrected upper limit column densities.

Table C.2 lists the column densities of the reference molecules  $H_2$ ,  $H_2O$ ,  $CH_3OH$ ,  $HF$ ,  $H^{35+37}Cl$  taken from [Crockett et al. \(2014a\)](#), [Neill et al. \(2014\)](#) and [Zernickel et al. \(2012\)](#).

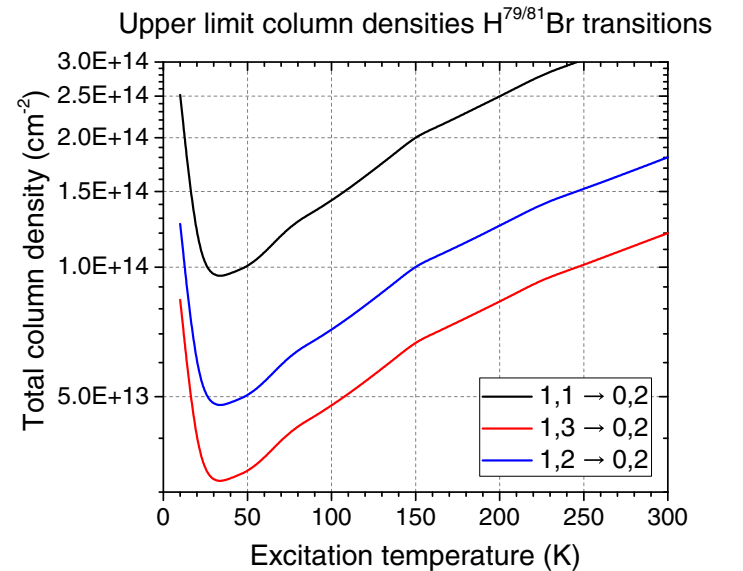


**Fig. C.1.** Upper limit column densities for the  $H^{79/81}Br$  (e.g.  $^{79}Br$  and  $^{81}Br$  are used interchangeably here)  $J = 1_x \rightarrow 0_2$  transitions plotted versus rotational temperature based on the  $3\sigma$  values ( $216 \text{ mK km s}^{-1}$ ) found for the Orion KL Hot Core and beam-dilution corrected ( $\eta = 0.049$ )

**Table C.1.**  $\text{H}^{79+81}\text{Br}$  column densities and beam dilution correction.

| Source         | $N_{\text{T}}(\text{H}^{79+81}\text{Br})$ ( $\text{cm}^{-2}$ ) |                           | $\eta_{\text{BF}}$     | $N_{\text{S}}$            |                           |
|----------------|--|---------------------------|------------------------|---------------------------|---------------------------|
|                | Emission*  | Absorption                |                        | Emission*                 | Absorption                |
| Orion KL Plat. | $\leq 7.9 \times 10^{12}$                                      | $\leq 1.1 \times 10^{14}$ | $3.2 \times 10^{-1}$   | $\leq 2.5 \times 10^{13}$ | $\leq 3.4 \times 10^{14}$ |
| Orion KL HC    | $\leq 4.7 \times 10^{12}$                                      | $\leq 3.8 \times 10^{13}$ | $4.9 \times 10^{-2}$   | $\leq 9.6 \times 10^{13}$ | $\leq 7.8 \times 10^{14}$ |
| Orion KL CR    | $\leq 4.3 \times 10^{12}$                                      | $\leq 3.3 \times 10^{13}$ | $4.9 \times 10^{-2}$   | $\leq 8.8 \times 10^{13}$ | $\leq 6.7 \times 10^{14}$ |
| Sgr B2(N) HC   | $\leq 6.7 \times 10^{12}$                                      | $\leq 4.0 \times 10^{13}$ | $1.3 \times 10^{-2}$   | $\leq 5.2 \times 10^{14}$ | $\leq 3.1 \times 10^{15}$ |
| Sgr B2(N) env. | $\leq 1.0 \times 10^{13}$                                      | $\leq 8.9 \times 10^{13}$ | –                      | –                         | –                         |
| NGC6334I HC    | $\leq 1.2 \times 10^{12}$                                      | $\leq 1.2 \times 10^{13}$ | $1.3 \times 10^{-2}$   | $\leq 9.2 \times 10^{13}$ | $\leq 9.2 \times 10^{14}$ |
| NGC6334I env.  | $\leq 1.7 \times 10^{12}$                                      | $\leq 2.4 \times 10^{13}$ | $1.7 \times 10^{-1**}$ | $\leq 1.0 \times 10^{13}$ | $\leq 1.4 \times 10^{14}$ |

**Notes.** (\*)Emission at  $T_{\text{ex}} = 100$  K; (\*\*)beam dilution factor based on  $\text{HC}\ell$  source size.

**Table C.2.** Column densities of the reference molecules  $\text{H}_2$ ,  $\text{H}_2\text{O}$ ,  $\text{CH}_3\text{OH}$ ,  $\text{HF}$ ,  $\text{H}^{35+37}\text{Cl}$ .

| Source                      | $\text{H}_2$         | $\text{H}_2\text{O}$          | $\text{CH}_3\text{OH}$<br>( $\text{cm}^{-2}$ ) | $\text{HF}$           | $\text{H}^{35+37}\text{Cl}$ |
|-----------------------------|----------------------|-------------------------------|--|-----------------------|-----------------------------|
| Orion KL Plat. <sup>a</sup> | $2.8 \times 10^{23}$ | $1.3 \times 10^{18}$          | –  | $2.9 \times 10^{13*}$ | $1.9 \times 10^{15}$        |
| Orion KL HC <sup>a</sup>    | $3.1 \times 10^{23}$ | $2 \times 10^{20}$            | $6.8 \times 10^{17}$                           |                       |                             |
| Orion KL CR <sup>a</sup>    | $3.9 \times 10^{23}$ | $1.8 \times 10^{18}$          | $4.7 \times 10^{17}$                           |                       |                             |
| Sgr B2(N) HC <sup>b</sup>   | $8 \times 10^{24}$   | $5\text{--}10 \times 10^{16}$ | $5 \times 10^{18}$                             |                       |                             |
| Sgr B2(N) env. <sup>b</sup> | –                    | –                             | $1 \times 10^{16}$                             | $8.2 \times 10^{14*}$ | $1.3 \times 10^{15*}$       |
| NGC6334I HC <sup>c</sup>    | $1.1 \times 10^{24}$ | $2.1 \times 10^{18}$          | $1.4 \times 10^{19}$                           | –                     | $1.9 \times 10^{14}$        |
| NGC6334I env. <sup>c</sup>  |                      |                               |  | $1.2 \times 10^{14*}$ | $1.5 \times 10^{14*}$       |

**Notes.** (a)Crockett et al. (2014a), (b)Neill et al. (2014) (c)Zernickel et al. (2012) and references therein; (\*)absorption component.